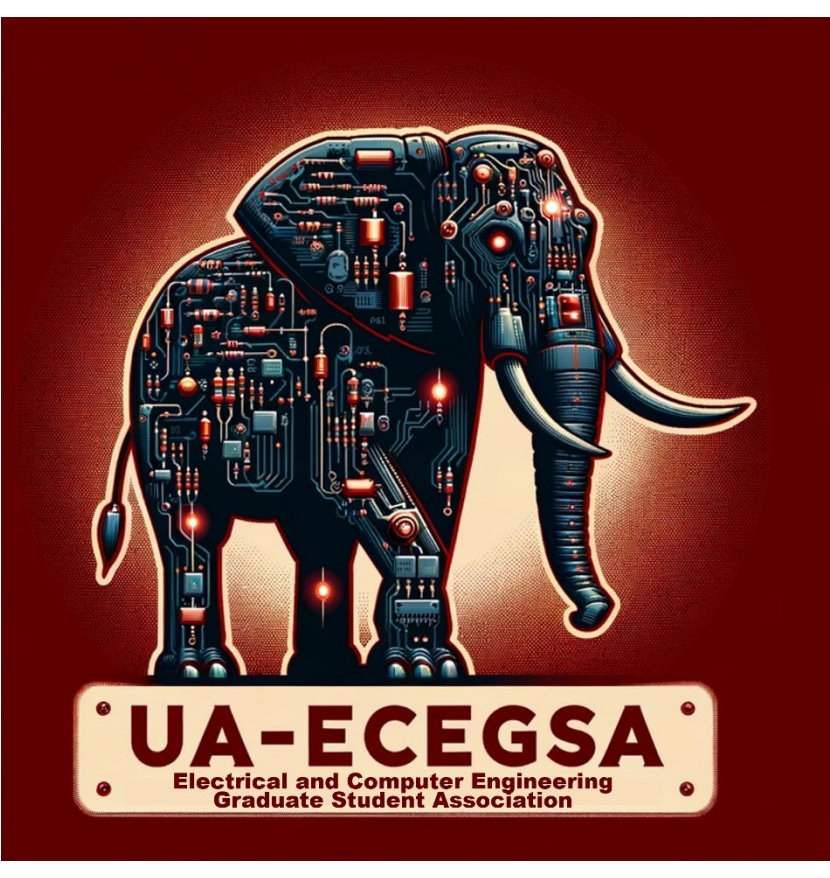
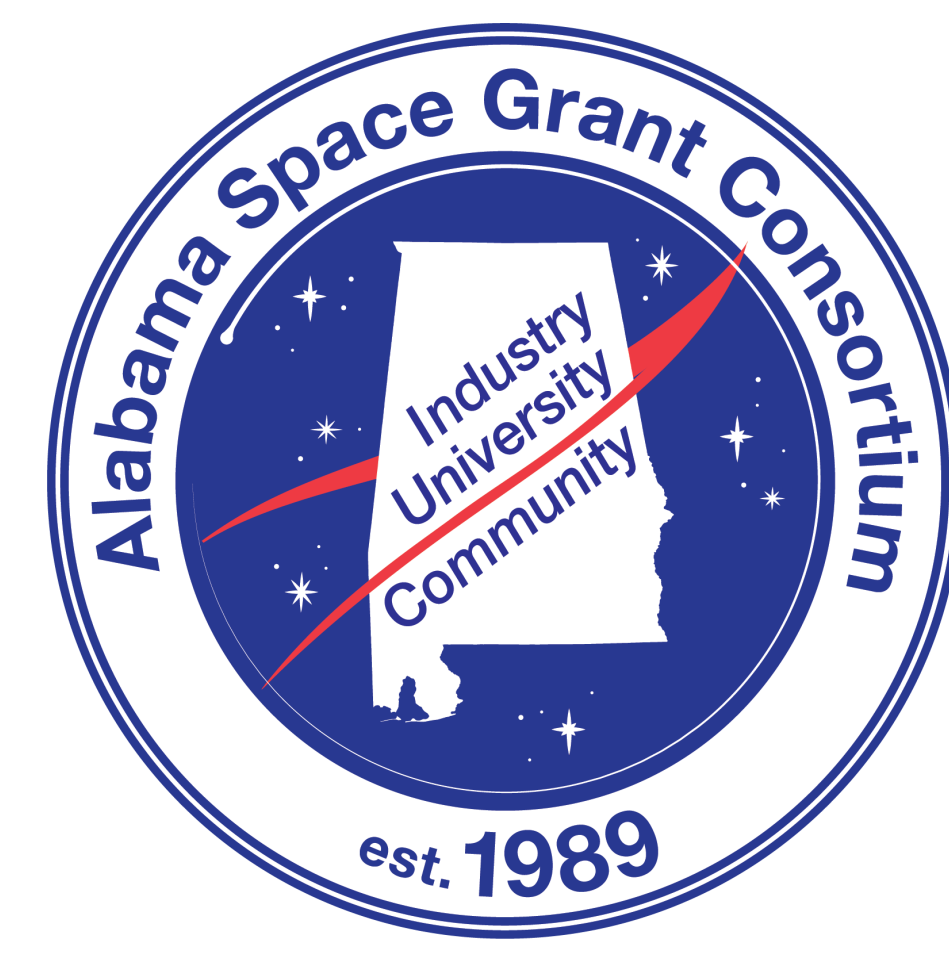


Design and Modeling of Ruggedized Agriculture RoBot (AgBot)

Lauren Ervin, Dr. Harish Bezawada, and Dr. Vishesh Vikas
Agile Robotics Lab, The University of Alabama



Introduction and Motivation

Tensegrities synergistically combine elements of tension (elastic cable) and compression (rigid, curved-link) elements to achieve structural integrity, providing a high strength-to-mass (S2M) ratio among other benefits. Consequently, they are lighter alternatives for interacting in unstructured environments. Due to their many advantages, researchers have garnered interest in creating continuum robot manipulators with tensegrity primitives. In fact, tensegrity manipulators exhibit a much higher S2M ratio than traditional robot manipulators.



Fig. 1: Robot Manipulator Motor Placement [1]
The agriculture robot shown on the top of Fig. 1 contains multiple actuators fixed to the arm joints. This creates significant weight that hangs away from the base, limiting the additional payload that the robot arm is capable of lifting. Traditional robot manipulators have a S2M ratio of 0.75:1 [2] whereas preliminary tests with AgBot, shown on the bottom of Fig. 1, show 3:1.

Contributions: AgBot, the Agriculture RoBot, is comprised of the following:

1. Two rigid, semi-circular curved links are held together with 12 elastic cable segments. This tensegrity primitive (based off a snub disphenoid) is hereby referred to as a vertebra and has a notch on each arc as a connection point.
2. 10 vertebra are connected in series to form a cable-driven tensegrity continuum manipulator that is controlled with four motor tendon actuators (MTA) at the base; this design provides balance between a high S2M ratio and stability.
3. The kinematics and geometric modeling of a single vertebra are shown.
4. Observable, non-linear behavior of the continuum manipulator is displayed.

Non-Commutative Behavior

The continuum manipulator exhibits non-commutative behavior in multiple ways:

1. For a set of two sequences, forwards and backwards, the backwards sequence will not end in the same position that the forward sequence started in.
2. When starting in the same configuration, the same set of commands performed in a different order results in two unique endpoints.

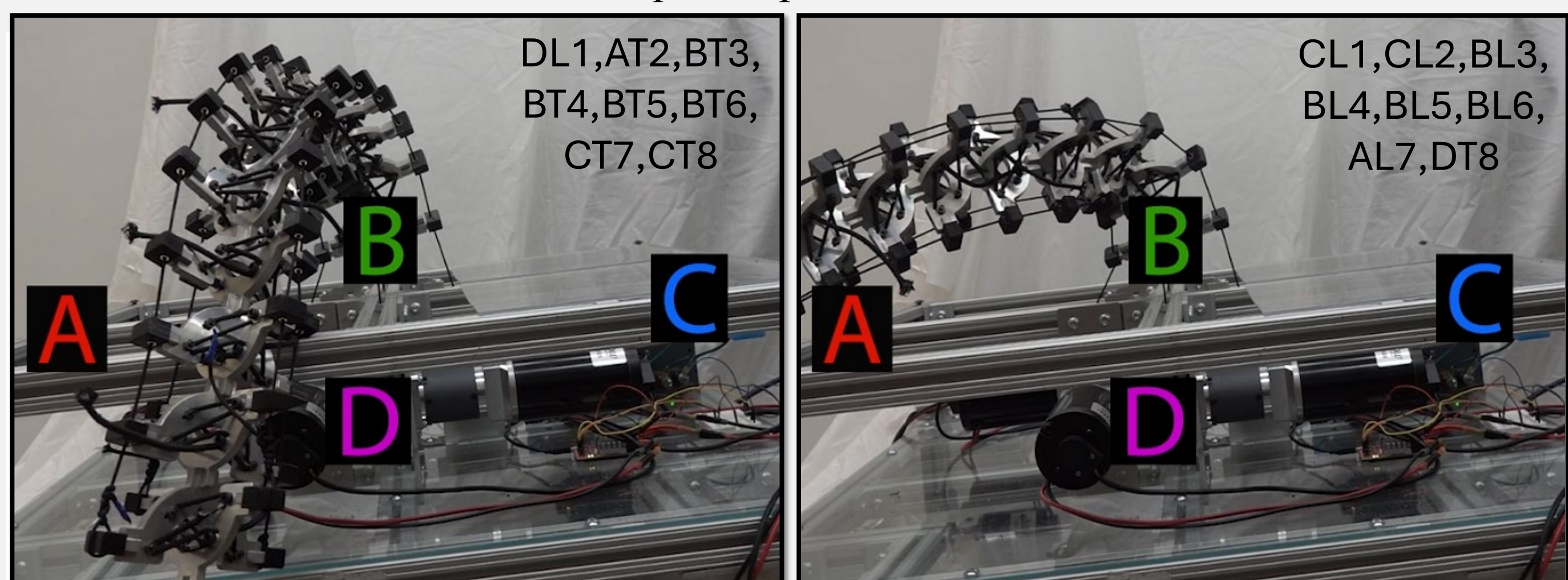


Fig. 4: Forward and Backward Sequences Resulting in Different End Positions



Kinematics and Dynamics of Single Vertebra and Continuum Manipulator

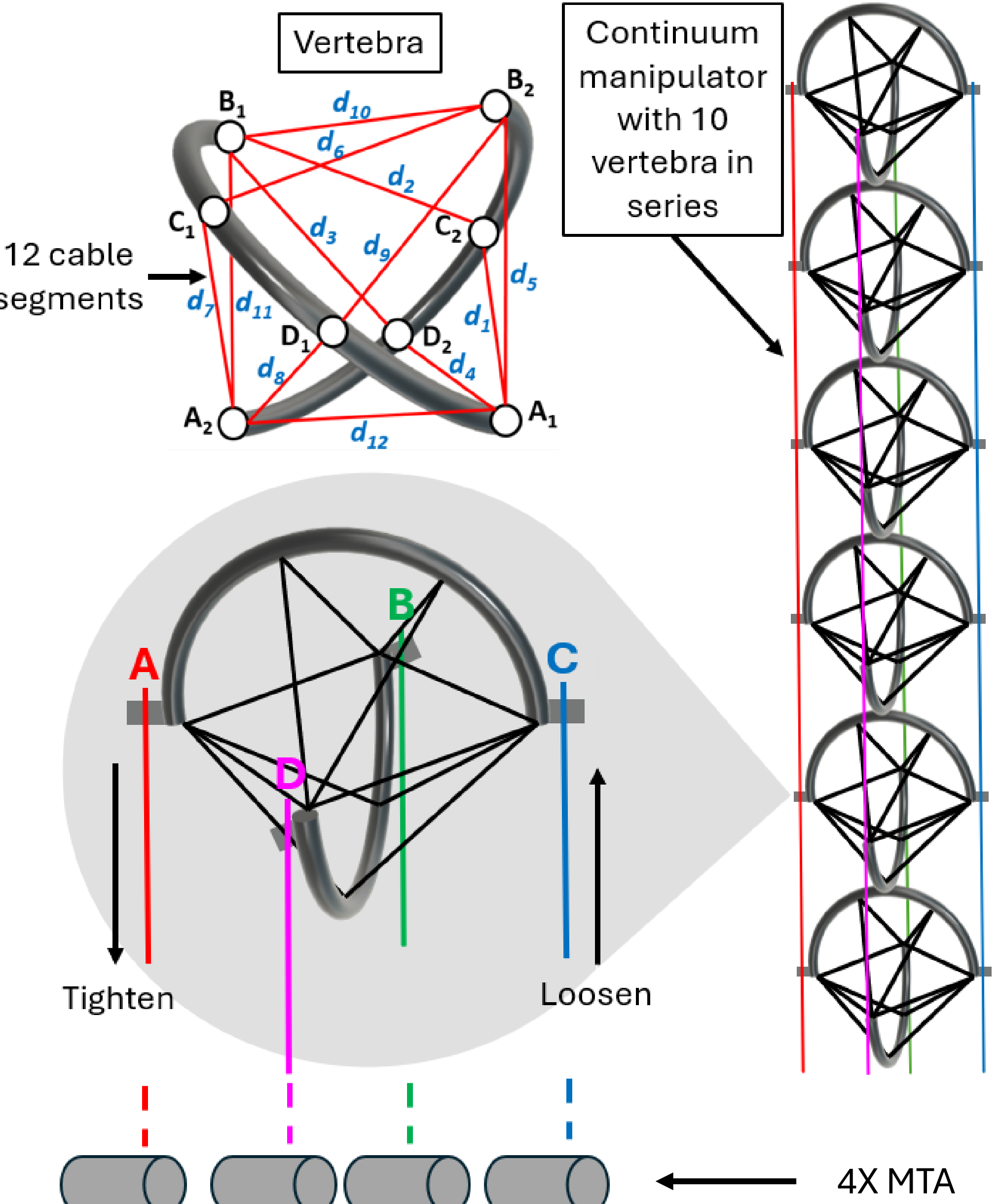


Fig. 2: Vertebra and Manipulator Geometric Representation

The continuum manipulator consists of 10 identical vertebra connected in series. The unique design of the vertebra in Fig. 2 poses static and dynamic modeling challenges:

1. A vertebra is a closed chain, but the manipulator is an open chain;
2. The MTA movement is non-linear, creating complex behavior.

There are four connection points on each curved-link in a vertebra expressed in the link coordinate systems and represented by $P \in \mathbb{R}^{4 \times 4}$. The connectivity matrices $C_1, C_2 \in \mathbb{R}^{4 \times 12}$ represent the two end connection points of each of the 12 cable segments, $D \in \mathbb{R}^{4 \times 12}$, where the i th cable \mathbf{d}_i is denoted by the i th column, and $|\mathbf{d}_i|$ is the Euclidean norm. The transformation matrix $T_{12} \in SE(3)$ transforms vectors from coordinate system {2} to {1} and is time-dependent. The body wrench \mathcal{F}_b is comprised of the linear and angular momenta from the string forces F_s , tendon forces F_t , and connection force F_m . This lets us dynamically solve for the body twist V_b in Fig. 3.

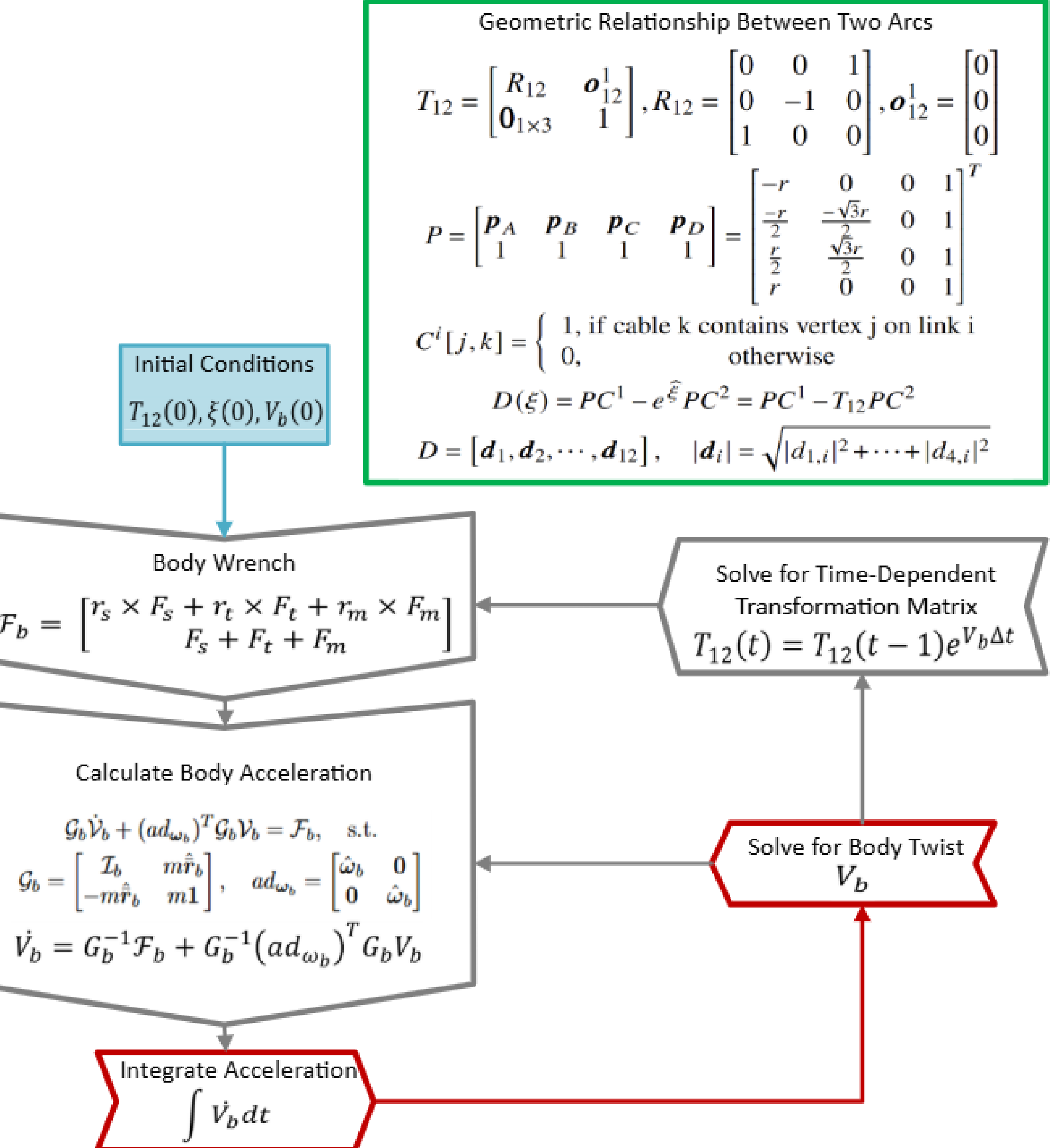


Fig. 3: Kinematics & Dynamics for Closed-Chain Vertebra

Mechatronics and Systems Integration

1. Mechanical Design:

Curved arcs comprising a vertebra were 3D printed with Onyx filament and held together with Nylon elastic cable. The vertebra were connected in series through connection points at the base of each arc and additionally secured with M2 screws. The continuum manipulator is cable-driven with four MTA consisting of IG52-04 brushed DC motors with 1:81 planetary gear boxes. The manipulator is fixed to a ruggedized, wheeled platform fabricated primarily out of 80/20 and driven with E30-150-24 brushed DC motors with 1:16 planetary gear boxes. The chassis houses the four MTAs, all electronics, and the LiPo battery and is covered with acrylic sheets to protect from outside elements during field testing in agriculture settings.

2. Electrical Design:

There are two primary PCBs designed for this, a data PCB and power PCB, that interface with all components.

- Data is collected from five BNO085 9-axis IMUs, one Intel RealSense L515 LiDAR camera, one RGB camera, and four in-line load cells. The IMUs measure the orientation and acceleration at different points along the manipulator, the LiDAR camera covers the entire manipulator, the RGB camera covers in front of the platform to help with object avoidance and path planning, and the load cells measure the tension along the four tendon paths. The IMU data is read via an I2C MUX, and the load cell data is read via HX711 ADCs. The data PCB is connected to a Jetson Orin Nano which serves as the controller of the system.
- Power is delivered to all system components through a power PCB from a 22.2V 10Ah LiPo. Power relays and fuses are connected to all motors to prevent excessive current draw. Pull-up resistors are used to interface with the encoders and filter capacitors are used to reduce noise in the system. Additionally, the RoboClaw motor controllers enable further current limiting. A voltage regulator drops VCC to 5V for all logic components on the data PCB. Finally, an E-stop is connected to increase the safety of the system.

3. Software Design:

The manipulator is currently manually driven with Circuit Python and an Xbox controller. ROS 2 Humble is installed on the system, and we plan to automate control through that as well as perform sensor fusion soon.

Future Works

- Finalize systems integration and testing.
- Perform field data collection.
- Perform shape estimation of the continuum manipulator.

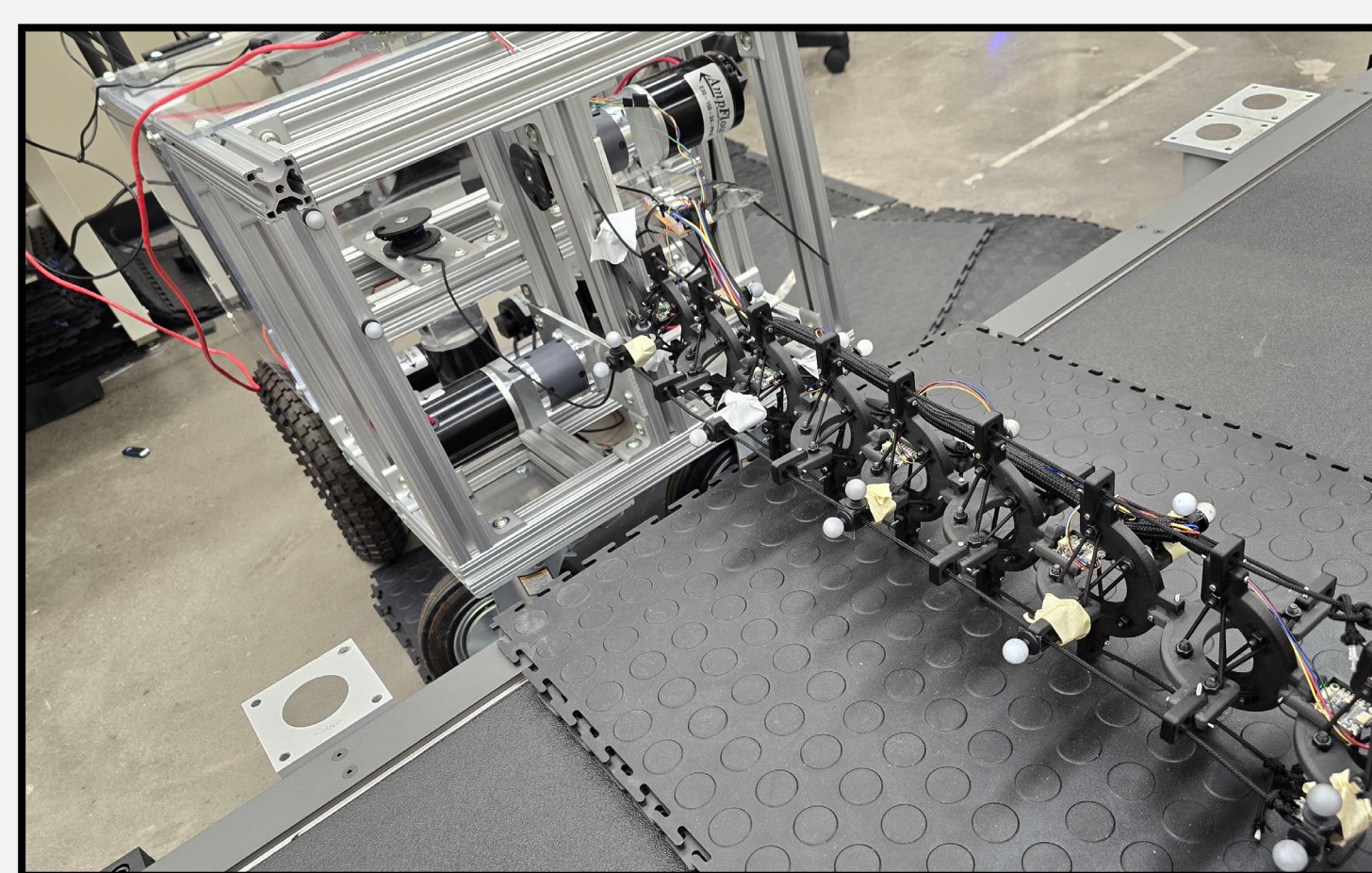


Fig. 5: Collecting GT VICON Data for Shape Reconstruction

References

1. Robotnik. (2022, June 15). Robotics applications in agriculture. Robotnik. <https://robotnik.eu/robotics-applications-in-agriculture/>
2. Merckaert, K., De Beir, A., Adriaens, N., Makrini, I. E., Van Ham, R., & Vanderborght, B. (2018). Independent load carrying and measurement manipulator robot arm for improved payload to mass ratio. *Robotics and Computer-Integrated Manufacturing*, 53, 135–140. <https://doi.org/10.1016/j.rcim.2018.04.001>